Pre-normative REsearch for Safe use of Liquid Hydrogen (PRESLHY)

Project Deliverable

Computational investigation of ignition phenomena related to cryogenic hydrogen

Deliverable Number:	D25 (D4.2)
Work Package:	4
Version:	1.0
Author(s), Institution(s):	D. Cirrone, V. Molkov, D. Makarov (UU)
Submission Date:	05/2021
Due Date:	06/2021
Report Classification:	Public

This project has received funding from the Fuel Cells and Hydrogen 2 Joint Undertaking under the European Union's Horizon 2020 research and innovation programme under grant agreement No 779613.

History		
Nr.	Date	Changes/Author
1.0 - Draft	20/05/2021	Original version

Approvals			
Version	Name	Organisation	Date
1.0 - Draft	Simon Coldrick	HSE	20/05/2021

Acknowledgements

This project has received funding from the Fuel Cells and Hydrogen 2 Joint Undertaking under the European Union's Horizon 2020 research and innovation programme under grant agreement No 779613.

Disclaimer

The data management in the PRESLHY project follows the principle of data management, which shall make data Findable, Accessible, Interoperable and Re-usable (FAIR). The plan for FAIR data management as described in this document is based on the corresponding template for open research data management plan (DMP) of the European Research Council (ERC).

Despite the care that was taken while preparing this document the following disclaimer applies: The information in this document is provided as is and no guarantee or warranty is given that the information is fit for any particular purpose. The user thereof employs the information at his/her sole risk and liability.

The document reflects only the authors' views. The FCH JU and the European Union are not liable for any use that may be made of the information contained therein.

Key words

Computational fluid dynamics, liquid hydrogen, ignition, combustion

Publishable Short Summary

Work package four of the PRESLHY project focuses on ignition phenomena. This report summarises computational modelling work which was carried out to complement the experimental programme. Three particular scenarios have been considered: firstly, the determination of the MIE in hydrogen-air mixtures at arbitrary composition and initial temperature; secondly, the effect of hydrogen temperature decrease on pressure limit leading to spontaneous ignition in a T-shaped channel and thirdly, the investigation of the condensation of oxygen over an evaporating LH2 pool and its potential to cause highly energetic events after ignition.

The CFD model was seen to predict accurately experimentally measured MIE for both ambient and cryogenic temperature hydrogen-air mixtures. Thus, the model can be used as a means of calculations of potential hazards in hydrogen safety engineering.

A LES approach was employed to investigate the effect of hydrogen temperature decrease on pressure limit leading to spontaneous ignition in a T-shaped channel. For cryogenic hydrogen (80 K), it was found that a pressure approximately 4 times larger than for warm hydrogen is required to trigger ignition and sustain combustion outside the T-shaped channel, which could likely lead to a hydrogen jet fire.

CFD modelling can be used to investigate the formation of cryogenic hydrogen and condensed oxygen mixtures. CFD simulations can be used to support experimental investigations where it may not be possible to exactly define the underlining cause of highly energetic events following combustion of cold hydrogen/oxygen mixtures.

Table of Contents

1 Introduction

Work package four of the PRESLHY project focuses on ignition phenomena. This report summarises computational modelling work which was carried out to complement the experimental programme. Three particular scenarios have been considered: firstly, the determination of the MIE in hydrogen-air mixtures at arbitrary composition and initial temperature (Section 2); secondly, the effect of hydrogen temperature decrease on pressure limit leading to spontaneous ignition in a T-shaped channel (Section 3) and thirdly, the investigation of the condensation of oxygen over an evaporating LH2 pool and its potential to cause highly energetic events after ignition (Section 4).

2 Numerical determination of MIE by spark ignition (UU)

Spark capacitive discharge is the most common technique to determine minimum ignition energy (MIE) for flammable mixtures in experiments (Kumamoto et al., 2011). From a safety point of view, it is the most common type of electrostatic discharge associated to ignition hazards (Pratt, 2000).

The MIE of a hydrogen-air mixture is reported as 0.017 mJ in proximity of the stoichiometric composition (ISO/TR 15916, 2004). This value is much lower than other flammable gases, such as methane or ethane, usually characterised by MIE greater than 0.1 mJ (Lewis and Von Elbe, 1961). The MIE changes depending on the oxygen content in the mixture, decreasing to a value as low as 0.0057 mJ for air containing 35% by vol. of oxygen (Kumamoto et al., 2011). MIE for mixtures of hydrogen-oxygen can hardly be measured by usual experimental apparatus. Kuchta (1985) reported a value as low as 0.0012 mJ.

The experimental apparatus may also affect the measured MIE, leading to up to twice difference for lean mixtures, as showed by (Kuchta, 1985) for comparison with data from (Lewis and Elbe, 1961) and (Calcote et al., 1952).

The scope of the present computation study is to develop and validate a CFD model capable to reproduce the MIE curve for several hydrogen concentrations and initial temperatures of the mixture. The novelty of the study is given by the employment of more accurate 3D simulations and the expansion of validation range to cryogenic mixtures.

The CFD modelling complements and supports the analytical modelling for determination of MIE performed by UU and presented in PRESLHY D6.5. The CFD model allows to give insights into the effect of the experimental apparatus features, e.g. the electrodes' size. Furthermore, it gives further insights into the dynamics of the process, flame kernel development, effect of conductive or radiative losses, etc.

Simulations results are compared against experiments performed by (Lewis and Elbe, 1961) and (Ono et al., 2007) for ambient temperature hydrogen-air mixtures. Experiments performed within PRESLHY project by INERIS (Proust, 2021) were used to assess the CFD model predictive capability at cryogenic temperatures.

2.1 CFD model, numerical details and assumptions

The CFD approach employs detailed chemical kinetics, including 13 chemical species and 37-step reduced chemical reaction for hydrogen-air combustion. The model takes account of radiation losses through the Discrete Ordinates method. A Courant Friedrichs Lewis number equal to 0.3 is imposed in calculations. The numerical formation process of the flame kernel is expected to be axisymmetrical, therefore only a quarter of a sphere with

radius 5 mm is used as numerical domain. The numerical grid has a total of approximately 138,000 control volumes. Simulations were performed for hydrogen concentration in air in the range 10-55%, as reported in Table 1.

It is assumed that the spark has duration 1 μs and all the nominal stored energy is available to ignite the mixture. Energy is released in a cylindrical channel with height equal to the spark gap and radius equal to 100 μm, following observations in (Benmouffok et al., 2018). For ambient temperature mixtures, the spark gap, i.e. the distance in between needle to needle electrodes, is varied in the range 0.5-2 mm depending on experimental tests by (Ono et al., 2007). Table 1 reports the electrodes gap considered for each tested concentration. The electrodes are tungsten cylindrical bars made with diameter 1 mm with a 40° angle tip. The tip diameter is 0.3 mm as in (Ono et al., 2007). The model takes account of conductive losses to the electrodes.

Table 1. Hydrogen concentration and electrodes gap in simulations for ambient temperature mixtures.

Test	H_2 by vol. in air, %	Electrodes gap, mm
1	10	2.0
2	14	1.0
3	22	0.5
4	29	0.5
5	35	1.0
6	45	1.0
6	55	2.0

For cryogenic temperature mixtures, the spark gap is equal to 0.5 mm, as in experiments by Proust (2021). Table 2 reports the hydrogen concentrations tested in simulations.

Table 2. Hydrogen concentration and electrodes gap in simulations for cryogenic temperature mixtures.

Test	H_2 by vol. in air, %	Electrodes gap, mm
1	20	0.5
2	30	0.5
3	40	0.5
4	60	0.5

2.2 Simulation results for ambient temperature mixtures

2.2.1 Determination of MIE

The minimum ignition energy is determined by progressively reducing the energy released in the spark channel and verify until which value released energy leads to ignition. The release of energy in a short time (spark duration is assumed to be 1 μs) causes a steep increase of temperature in the spark channel to values that could reach 10000 K (Terao, 2007). After stopping the release energy, temperature quickly decreases because of losses and mixing with the fresh mixture. In simulations the ignition is considered to verify when there is formation of a flame kernel propagating outwards the spark channel. Presence of hydroxyl (OH) radical mole fraction, accumulation of combustion products (water vapor) and high temperatures are used as indication of a successful ignition. The following criteria are considered to determine the ignition failure: decrease of temperature below 600 K, lack of sustainment of OH radical production and absence of water vapour accumulation in the domain.

Figure 1 shows the ignition energies resulting in ignition or failure to ignite in simulations for the cases reported in Table 1. The absolute MIE is found for hydrogen concentration in air 22 and 29% by vol and is equal to 15 μJ. Conversely, the mixtures fail to ignite for IE= 12 μJ. Simulation results well reproduce experimental measurements and widely accepted MIE of 17 μJ. The CFD model is extended to the assessment of MIE for lean and rich hydrogen-air mixtures by changing the spark gap accordingly. Simulated ignition energies for hydrogen concentrations 10 and 14% by vol in air for spark gaps 2 and 1 mm respectively, perfectly agree with experimental measurements by (Ono et al., 2007). For rich mixtures, simulations conservatively predict experimental measurements. This may be due to an increase of ionisation losses, which would increase for increasing released energy (Jarosinski and Veyssiere, 2009), which are not taken into account in the numerical modelling. Overall, it is found that simulations results well predict experimental measurements within the range of hydrogen concentrations 10-55 % by vol in air.

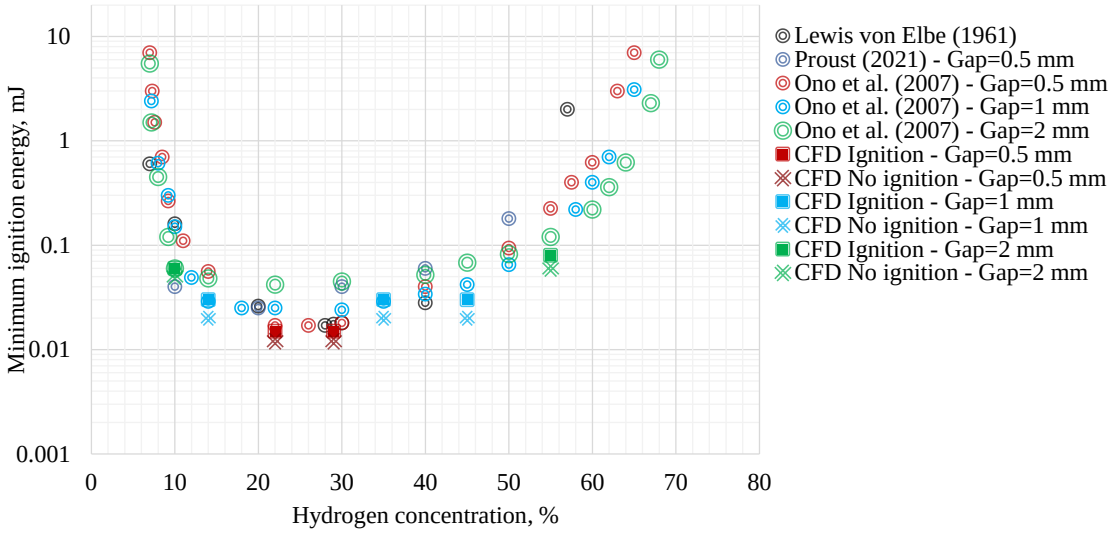

Figure 1. Comparison of CFD calculations of MIE in hydrogen-air mixture with initial temperature 288 K against experiments by Ono et al. (2007), Lewis & von Elbe (1961) and Proust (2021).

2.2.2 Evolution of a flame kernel

The simulation results can give insights into the flame kernel growth process. Figure 2 shows the spark channel at 1 μs, which is assumed to be the spark duration. The ignition energy used in this case was 15 μJ, which is the MIE determined in numerical simulations. Temperature is within 2300 K and maximum OH mole fraction is of the order of 10^{-6}.

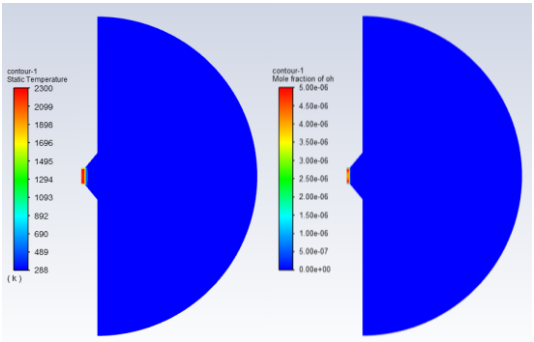

Figure 2. Spark channel at 1 μs for T=288K, H_2=29% by vol. in air, MIE=15μJ.

Figure 3 shows the flame kernel growth from 45 to 500 μs via the temperature and OH mole fraction contours. At 45 μs the high temperature zone is mainly located at the centre of the spark, due to the effect of losses to the electrodes. The flame kernel starts to develop at 100 μs, as shown by the increasing presence of OH specie. Beyond this time, the flame starts to expand spherically. Figure 4 shows the distribution of temperature and OH mole fraction along the direction perpendicular to the spark channel axis. Flame front temperature establishes at about 2200K, which is slightly lower than adiabatic flame temperature (2388 K) due to presence of losses by conduction to the electrodes and by radiation. OH mole fraction distributions provide an indication of the reacting zone and, thus, of the flame front location. Simulation results indicate that the burning velocity is approximately 12 m/s.

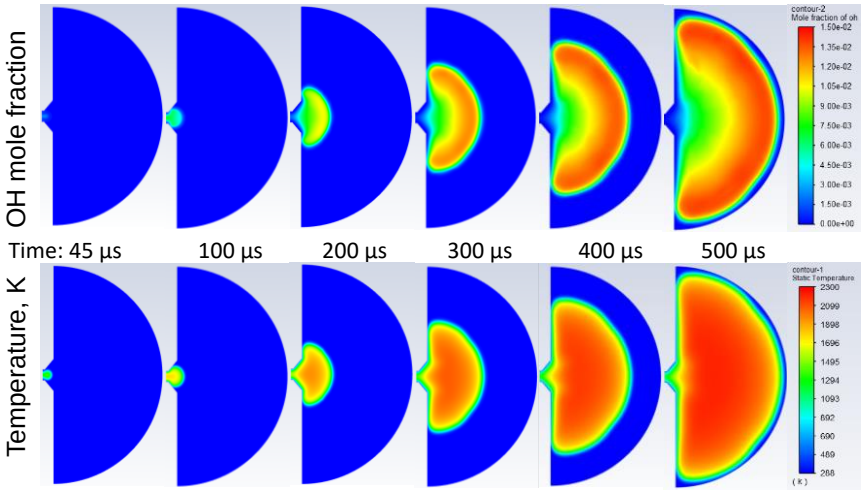

Figure 3. Flame kernel growth for T=288K, H_2=29% by vol. in air, MIE=15μJ.

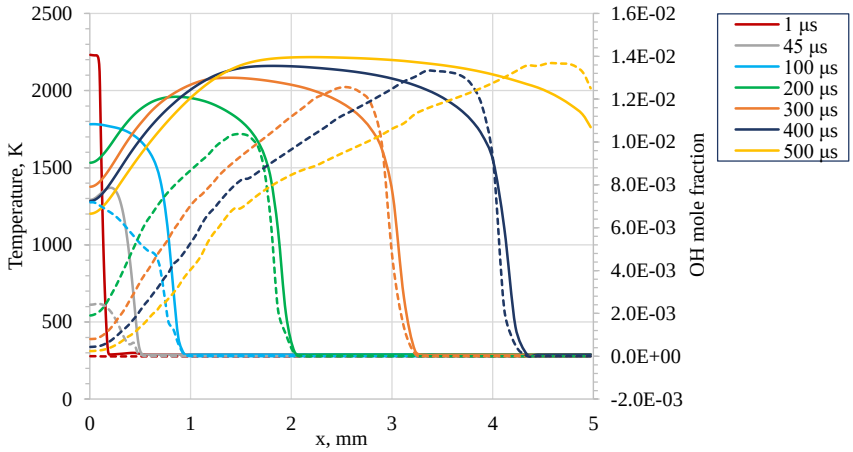

Figure 4. Temperature (solid lines) and OH mole fraction (dashed lines) distribution along direction perpendicular to the spark channel axis for T=288K, H_2=29% by vol. in air, MIE=15μJ.

2.2.3 Effect of numerical and experimental parameters

A CFL sensitivity test was conducted by decreasing its value from 0.3 to 0.1. Temperature distribution along the axis was used to assess the effect of CFL change. CFL=0.1 resulted in a slightly faster flame front. Variation was below 4.5% at 150 μs, which is considered to be acceptable. Thus, a CFL=0.3 was maintained to decrease simulations time.

The heat losses to the electrodes were investigated by analysing two limiting configurations with and without inclusion of electrodes with 1 mm diameter in the domain. It was found that the effect of electrodes presence on ignition energy was noticeable for lean hydrogen-air mixtures and for a spark gap of 0.5 mm. No variation was observed for a spark gap of 2 mm, which is comparable to the quenching distance for 10% H_2 by vol. in air (Kim et al., 2001). Thus, CFD simulation results align with conclusions by (Han et al., 2011) on the effect of the electrodes size for spark gaps below the quenching distances. A second analysis was performed on mixture with 10% H_2 by vol in air and a spark gap of 2 mm by changing the electrodes tips diameter from 1 mm to 0.2 mm. It was observed that a larger electrodes diameter would lead to a lower temperature and OH maximum mole fraction during the spark discharge. This may potentially lead to a different ignition limit for low energy discharges.

During the spark discharge, temperatures higher than 10000 K may occur (Terao, 2007). At these temperatures, significant radiation losses may occur. UU conducted a CFD study to analyse their effect, comparing two limiting cases with and without radiation modelling. The gas in the spark channel was assumed to have emissivity equal to 1, given that the high temperature plasma can be treated as a black body radiation source (Yang, 2011). The rest of the mixture was treated as per hydrogen jet fires in (Cirrone et al., 2019). It was showed that radiation losses affect significantly the maximum temperature reached in the spark channel. However, the MIE for a 10% H_2 mixture and spark gap of 0.5 mm was not affected by the inclusion of radiation modelling. The MIE was calculated by halving the energy released in the spark channel. A more gradual decrease in the energy discharge in simulations, may lead to a more accurate determination of MIE and a noticeable effect of radiation losses.

2.3 Simulation results for cryogenic temperature mixtures

Same procedure as for ambient temperature mixtures was applied here to retrieve MIE in cryogenic hydrogen-air mixtures. CFD modelling was performed for H_2 concentration 20-60% by vol. in air. Figure 5 shows the comparison of numerically determined MIE to experiments performed by (Proust, 2021) within PRESLHY project for an initial temperature of 173 K. All ignition energies leading to ignition of the mixture in experiments are displayed, regardless of a statistical analysis. The minimum energy leading to ignition is 30 μJ, whereas an energy discharge of 23 μJ is seen to not be sufficient to ignite the mixture. As expected, the numerical MIE increases with the decrease of temperature, precisely from 15 μJ for T=288 K to 30 μJ for T=173 K. The calculated MIE well agrees with experiments for the range of concentrations 20-30% H_2 by vol in air. For H2=40% by vol, the model results in an ignition energy lower than the minimum value recording ignition in experiments. However, it can be observed that a lower number of tests was performed for this concentration and may not be sufficient to withdraw exact conclusions on the accuracy of the analytical model predictive capability. At this concentration, the numerically determined IE, 30 μJ, well agrees with analytical prediction of 35 μJ (see PRESLHY D6.5). Simulations were performed for hydrogen-air mixtures with initial temperature 123 K. The MIE was found for 20-30% H2 by vol in air mixture and was equal to 40 μJ.

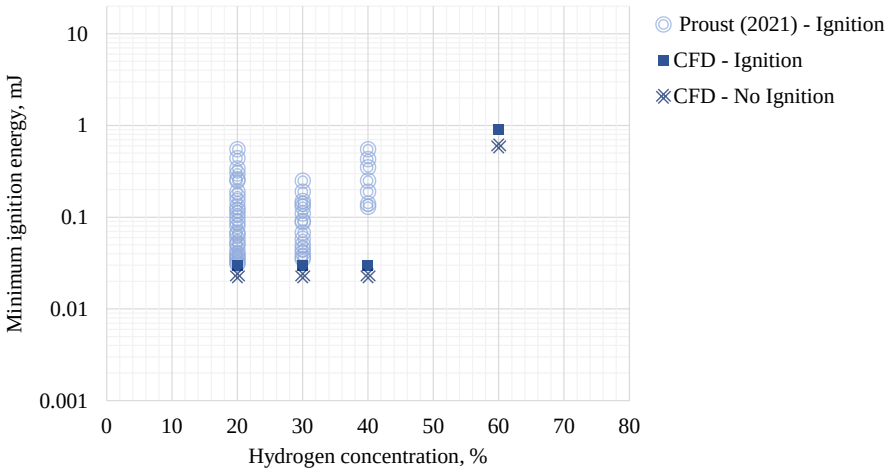

Figure 5. Comparison of CFD calculations of MIE in hydrogen-air mixture with initial temperature 173 K against experiments by Proust (2021).

Figure 6 shows the temperature and OH mole fraction contours on the symmetry plane for the time range 50-660 µs. The flame expands almost spherically with some disturbances of the flame front, which were not visible for ignition in ambient temperature hydrogen-air mixtures (see Figure 3). This may be indication of combustion instabilities which are enhanced for low temperature mixtures. The flame reaches the domain boundaries in 660 µs, which is a slightly larger time than observed for ambient temperature mixtures (500 µs). Figure 7 shows the distribution of temperature and OH mole fraction along the direction perpendicular to the spark channel axis. During the spark discharge (time 1 µs) the recorded maximum temperature is 4000 K (not visible in figure). Temperature quickly decreases because of losses and starts to increase again during flame propagation. Flame front temperature establishes at about 2100K, which is slightly lower than adiabatic flame temperature (2323 K) due to presence of losses by conduction to the electrodes and by radiation. Simulation results showed an increasing trend of the burning velocity, which reached 9.9 m/s at 500 µs. However, this was seen to not be established yet, and a larger domain should be used to better assess its value.

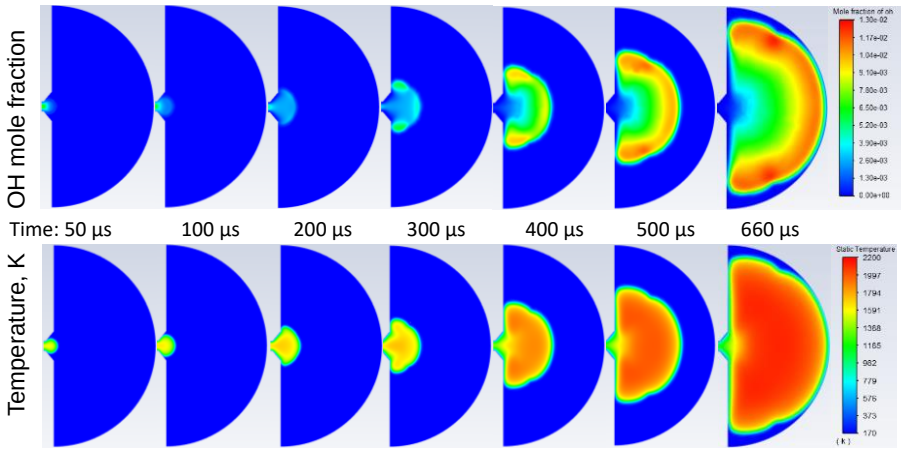

Figure 6. Flame kernel growth for T=173K, H2=30% by vol. in air, MIE=30µJ.

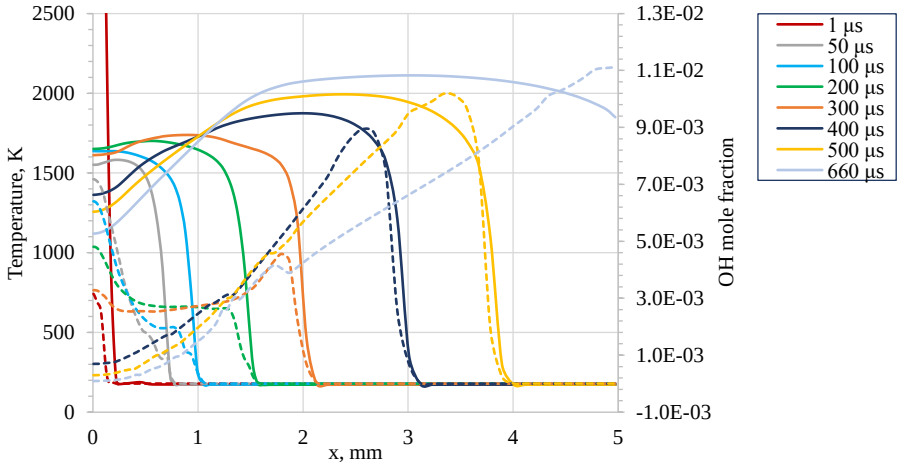

Figure 7. Temperature (solid lines) and OH mole fraction (dashed lines) distribution along direction perpendicular to the spark channel axis for T=173K, H2=30% by vol. in air, MIE=30µJ.

2.4 Conclusions

A CFD approach to numerically determine the MIE in hydrogen-air mixtures at arbitrary composition and initial temperature was developed and validated against experiments available in literature and against tests performed within PRESLHY project. The following conclusions are withdrawn for computational studies on ignition by spark:

- The CFD model was seen to predict accurately experimentally measured MIE for both ambient and cryogenic temperature hydrogen-air mixtures. Thus, the model can be used as a mean of calculations of potential hazards in hydrogen safety engineering.
- The numerically determined MIE was observed to increase with the decrease of temperature, in agreement with experimental and theoretical observations. It is considered that safety measures and strategies actuated for ambient temperature mixtures may be applicable to cryogenic mixtures, being conservative.
- Heat losses to the electrodes were found to affect simulation results, therefore these should be included into the CFD model and a configuration as close as possible to experimental should be considered by modellers.
- Experimental evidences showed that the MIE depends on the gap in between electrodes. It is important that simulations would reproduce exact experimental configuration to accurately predict MIE.
- Radiation losses were found to affect greatly the temperature reached during high energy discharges and these may affect the IE and flame propagation process.

The conclusions reported above are valid for ignition of hydrogen in normal air composition (21% by vol. O_2, 79% by vol. N_2). However, it is well known that ignition energy depends on the oxygen content in the mixture. This parameter rises in significance in the case of spurious LH_2 or cryogenic releases, where a local enrichment of oxygen can be reached due to the low temperature of the mixture. This effect should be carefully considered when evaluating the potential to ignite of cold hydrogen-air mixtures.

3 Diffusion ignition (UU)

A sudden hydrogen release from a high-pressure vessel can be spontaneously ignited. This mechanism has been firstly postulated by (Wolanski and Wojcicki, 1973), following their observations on ignition occurrence when high pressure hydrogen was admitted to a shock tube filled with air or oxygen. The authors suggested that ignition was caused by the high temperature gradient at the contact surface where the oxygen heated by the primary shock wave produced by the expanding gas, mixed and reacted with hydrogen due to diffusion. (Golub et al., 2007) investigated experimentally the effect of hydrogen pressure and release orifice size on verification of spontaneous ignition. It was found that a shock tube diameter should be larger than 3 mm for occurrence of ignition at hydrogen pressure between 150 and 400 bar and ambient temperature. The authors observed a strong dependence of spontaneous ignition parameters on the initial temperature. For hydrogen pressure equal to 200 bar, an increase of temperature from 300 K to 400 K caused a decrease in minimum release diameter leading to ignition from 3 mm to 2 mm. Similar conclusions were reached by (Bazhenova et al., 2006), who showed that an increase of initial temperature may cause an earlier ignition and verification for lower pressures. Further experiments were conducted by (Golub et al., 2008) to find the limit pressure for ignition in tubes of different lengths and cross-sectional shapes. The test on a tube with 5 mm diameter and 65 mm extension was selected in (Bragin and Molkov, 2011) for CFD modelling by using a Large Eddy Simulation (LES) approach. The minimum pressure storage leading to spontaneous ignition was found to be 20.4 bar.

It is expected that a decrease of temperature of compressed hydrogen to cryogenic would require a higher pressure to obtain spontaneous ignition. To the author's knowledge no experiments or numerical studies are available in literature for hydrogen at cryogenic temperature. The present study aims at fulfilling this knowledge gap by using CFD modelling to assess the effect of temperature decrease from ambient to cryogenic (80 K) on the ignition and combustion dynamics, determining the limit pressure leading to ignition and sustained combustion of the hydrogen jet. The CFD study is conducted on hydrogen spontaneous ignition in a T-shaped channel filled with air following an inertial flat burst disk rupture. Results will be used to understand the impact of enhanced density of cryogenic releases on the shock ignition process, and the trade off against increased difficulty of igniting cold H_2/air mixtures.

3.1 Simulation scenario

The case selected for the analysis is the sudden release of hydrogen from a high-pressure system into a T-shaped channel following the inertial flat burst disk rupture mimicking a Pressure Relief Device (PRD). The geometry of the release system is based on the experimental test conducted in (Golub et al., 2010) and numerically simulated in (Bragin et al., 2013). The release system is shown in Figure 8. The high pressure system is composed by a 210 mm long tube with 16 mm internal diameter (ID), connected to a 280 mm long tube with 10mm ID. The flat burst disk is located at the end of the high pressure tube and once ruptured releases hydrogen into the mock-up PRD open to atmosphere. The PRD consists of an axial channel with length 48 mm and diameter 6.5 mm. The PRD has a flat end where two radial channels are located. These vent hydrogen in the open atmosphere and have 6.25 mm length and 4 mm ID. Full description of the release system and geometry is available in (Bragin et al., 2013).

Simulations are performed for both ambient and cryogenic temperature to find the limit pressure leading to ignition. Table 3 shows the matrix of simulations. Results for ambient temperature hydrogen are compared to experimental and numerical test performed in (Golub et al., 2010) and (Bragin et al., 2013) respectively. Light sensors were used in experiments to register occurrence of spontaneous ignition. (Bragin et al., 2013) reported that no ignition was recorded for pressure equal to 1.2 MPa, whereas light was registered for 2.43 and 2.9 MPa.

Table 3. Selected scenarios for simulations.

N. simulations	Temperature, K	Pressure, MPa
6	300	1.35, 1.65, 2.43, 2.60, 2.80, 2.90
5	80	5.00, 7.00, 8.75, 9.40, 10.00

3.2 CFD model and numerical details

The CFD approach is based on the numerical work performed in (Bragin et al., 2013), with exception of the combustion model selected for the analysis. A LES approach is applied to simulate spontaneous ignition. Simulations have been conducted on Ansys Fluent v17.2. The CFD approach solved the conservation equations for mass, momentum, energy and species. The renormalization group (RNG) theory was used to model turbulence, given its capability to reproduce turbulent, transitional and laminar flows (Yakhot and Orszag, 1986). The finite rate chemistry model was used for combustion, which choice was justified by the small control volume size throughout the numerical grid. Hydrogen combustion in air was represented by a subset of 37 elementary chemical reactions and 18 species.

Details of the numerical domain are shown in Figure 8a. A control volume (CV) size equal to 200 μm was used in the zone of intersection between the axial and radial channels of the PRD. CV size of 250 μm was employed at the burst bisk whereas 400 μm was maintained in the PRD axial channel. CV size was increased to 10 mm in the far field of the PRD. The total number of cells was 417,685.

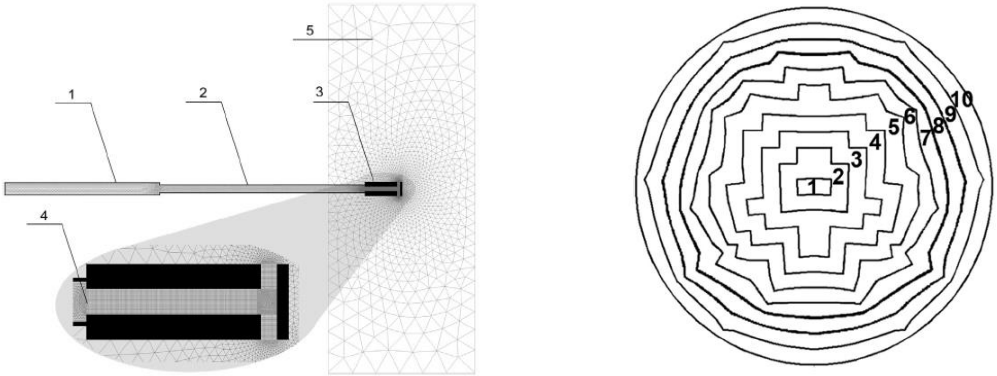

(a) (b)

Figure 8. a) The geometry and computational domain: 1 and 2 - high-pressure tubes, 3 - PRD, 4 - burst disk, and 5 – external domain (Bragin et al., 2013); b) Step-like approximation of a burst disk rupture process: 1-10 are sections that open in series (Bragin et al., 2013).

The external domain limit was modelled as non-reflecting pressure far field boundary. Tube walls were modelled as no-slip isothermal surfaces for the case with ambient temperature hydrogen, whereas they were modelled as coupled-walls made of steel for the case with cryogenic hydrogen. Hydrogen properties at cryogenic temperature, as the specific heat at constant pressure, were defined as function of data extrapolated from NIST database in (Bell et al., 2014). The domain was initialised with air of composition 0.23 and 0.77 in

oxygen and nitrogen mass fractions respectively. Temperature and pressure were initialized as 300 K and 101325 Pa respectively. The high-pressure tube was patched with hydrogen mass fraction equal to 1, pressure and temperature as in Table 3. An explicit method was used to solve governing equations and a four step Runge Kutta algorithm was employed for time advancement of simulations. The time step was determined from an imposed Courant Friedrichs Lewy (CFL) number of 0.3. A second-order upwind scheme with AUSM flux splitting was applied for flow discretisation.

Bragin et al. (2013) highlighted the importance of modelling the inertial opening of the membrane as it was found to generate more intense mixing between hydrogen and air, and affect the temperature of the shock heated air. The authors simulated the non-instant membrane opening by subdividing the flat burst disk in 10 sections (see Figure 8b) and by opening them in sequence. The same technique was employed in the present study. The opening time, *t*, was calculated as in (Spence and Woods, 1964):

$$t = k\left(\frac{\rho b d}{P}\right)^{1/2}$$

where k is a constant equal to 0.92 (range 0.91-0.93), ρ is the density of the diaphragm material, assumed to be annealed copper (8900 kg/m^3); b and d are the thickness and diameter of the diaphragm and P is the rupture pressure. The membrane opening time for each of the simulated rupture pressures is given in Table 4.

Table 4. Opening times of sections for simulated cases.

Section N.	1	2	3	4	5	6	7	8	9	10
Pressure, MPa	Opening time, μs									
1.35	0	4.7	9.5	14.2	18.9	23.7	28.4	33.1	37.9	42.6
1.65	0	4.2	8.6	12.8	17.1	21.4	25.7	29.9	34.3	38.5
2.43	0	3.5	7.1	10.6	14.1	17.7	21.2	24.7	28.3	31.7
2.5	0	3.4	7.0	10.4	13.9	17.4	20.9	24.3	27.9	31.3
2.6	0	3.4	6.9	10.2	13.6	17.1	20.5	23.8	27.3	30.7
2.7	0	3.3	6.7	10.0	13.3	16.8	20.1	23.4	26.8	30.1
2.8	0	3.3	6.6	9.9	13.1	16.5	19.7	23.0	26.3	29.6
2.9	0	3.2	6.5	9.7	12.9	16.2	19.4	22.6	25.9	29.1
5.0	0	2.4	4.9	7.4	9.8	12.3	14.8	17.2	19.7	22.1
7.5	0	2.0	4.0	6.0	8.0	10.1	12.0	14.0	16.1	18.1
8.75	0	1.8	3.7	5.6	7.4	9.3	11.2	13.0	14.9	16.7
9.4	0	1.8	3.6	5.4	7.2	9.0	10.8	12.5	14.4	16.1
10.0	0	1.7	3.5	5.2	6.9	8.7	10.4	12.2	13.9	15.6

3.3 Results and discussion

The scope of the computational study is to find the limit pressures providing spontaneous ignition and leading to a sustained combustion of the hydrogen jet. Temperature and hydroxyl (OH) mole fraction profiles are assessed to this scope and to give insights into the ignition dynamics. OH mole fraction is generally used to characterise the reacting zones in hydrogen-air flames. Results are presented for both ambient and cryogenic temperatures.

For ambient temperature hydrogen, an initial storage pressure in the range 1.35 MPa-2.9 MPa has been investigated. Pressure equal to 2.43 MPa did not lead to ignition. Figure 9 shows the temperature profile across the symmetry plane of the axial channel. Maximum

temperature reaches approximately 1500 K, which in combination with the shock pressure, is not enough to lead to ignition. This is confirmed by the maximum hydroxyl mole fraction dynamics in time, which, as shown in Figure 10, does not reach a significant value indicating combustion, but is rather negligible during the simulated time (up to 90 μs). Results for P=1.35 and 1.65 MPa are not showed as leading to similar results as 2.43 MPa.

The lack of ignition for pressure equal to 2.43 MPa somehow differs from numerical study in (Bragin et al., 2013) where ignition was recorded and combustion initiation was observed, even if the latter was rather weak and later self-extinguished. Experiments also confirmed numerical study, by recording ignition for this pressure (Golub et al., 2010).

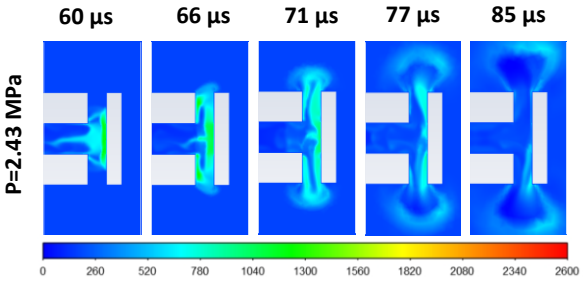

Figure 9. Temperature profiles across the symmetry plane for P=2.43 MPa. Ambient temperature hydrogen (300 K).

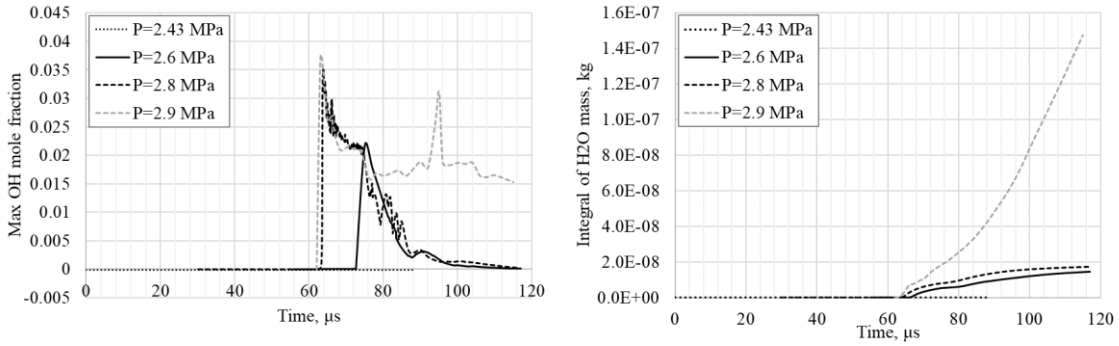

Figure 10. Time dynamics of maximum hydroxyl mole fraction (left) and integral of water vapour mass (right) across the domain. Ambient temperature hydrogen (300 K).

To find the limit providing ignition, the initial pressure was increased to 2.6 MPa. Figure 11 shows the temperature and hydroxyl mole fraction in time range 62-75 μs. It is possible to observe that temperatures up to 2600K are reached in the radial channels of the PRD. At the same spot there is recording of OH mole fraction starting at about 67 μs. Figure 12 focuses on the combustion dynamics outside the PRD and shows how OH mole fraction has completely disappeared from the symmetry plane by 90 μs. To provide a full overview of the reacting zone, Figure 13 shows the volumetric distribution of OH mole fraction above a limit of 0.001, which is generally accepted as delimitation for a reacting zone in combustion of hydrogen-air flames (Bulewicz and Sugden, 1958). This view could give insights into any reacting zone not located on the symmetry plane. It could be observed that at 90 μs, combustion is present in a small zone just outside the bottom radial channel, and that at 110 μs this has completely disappeared. The described dynamics is confirmed as well by the trend in time of the maximum OH mole fraction recorded in the domain (see Figure 10). Therefore, numerical simulation provided ignition at pressure equal to 2.6 MPa, followed by self-extinction of combustion. This is considered to predict within acceptable engineering accuracy the pressure limit of 2.43 MPa as observed in experiments for ignition. Numerical simulation for initial pressure equal to 2.8 MPa presented slightly

larger and longer presence of ignition and combustion zones, but also in this case there was self-extinction of the flame.

Also for initial storage pressure equal to 2.9 MPa, combustion is seen to be initiated in the bottom radial channel of the PRD (see Figure 11). A larger high temperature zone can be observed for P=2.9 MPa, with combustion initiated in a few localised spots as shown by OH mole fraction. These mainly depends on the hydrogen concentration in those locations, which is deemed to be closer to stoichiometric. Combustion later developed into a cocoon outside the PRD, leading to sustained combustion and likely transition into a jet fire (see Figure 12). Combustion is confirmed by the continuous presence of OH and the increase of water vapour integral in the domain (see Figure 10). External combustion is seen to be more enhanced towards the bottom side of the PRD and this is deemed to be caused by the inertial opening of the membrane. Simulation results well agree with experimental and numerical evidences in (Golub et al., 2010) and (Bragin et al., 2013), which showed ignition and combustion for P=2.9 MPa.

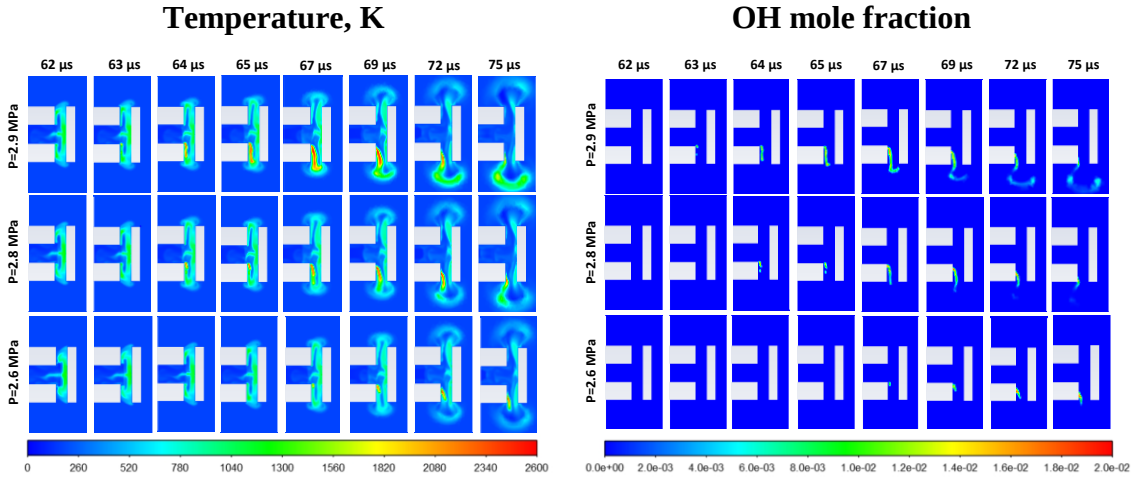

Figure 11. Temperature and hydroxyl mole fraction profiles for P=2.6, 2.8 and 2.9 MPa in time range 62-75 µs. Ambient temperature hydrogen (300 K).

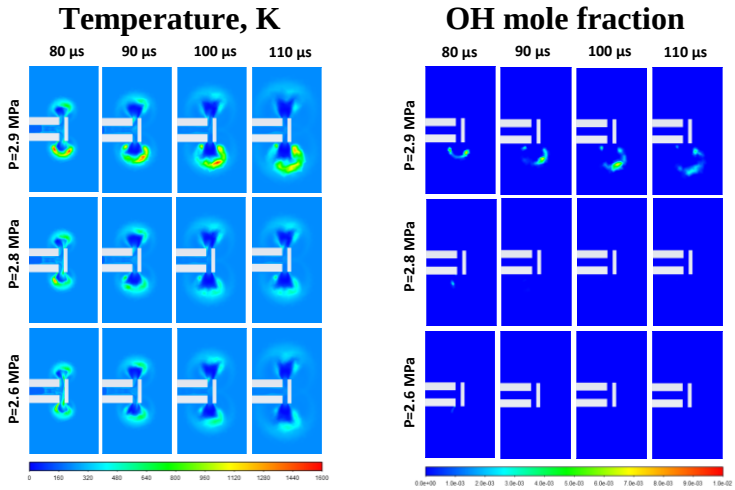

Figure 12. Temperature and hydroxyl mole fraction profiles for P=2.6, 2.8 and 2.9 MPa in time range 80-110 µs. Ambient temperature hydrogen (300 K).

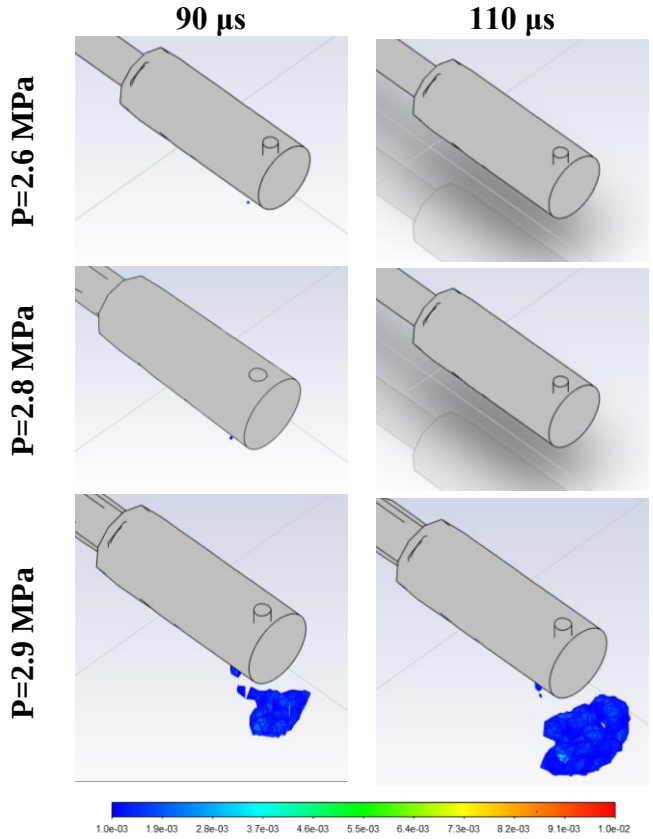

Figure 13. Hydroxyl mole fraction 3D distribution for P=2.6, 2.8 and 2.9 MPa. Ambient temperature hydrogen (300 K).

The same model and procedure were applied to determine the pressure limit for hydrogen stored at cryogenic temperature (80 K). The initial storage temperature was changed in the range 5-10 MPa. Figure 14 shows the temperature and hydroxyl profiles across the symmetry plane for pressures 7.5, 8.75 and 9.4 MPa, being the pressures closer to the recorded limit. Asymmetrical distribution of temperature at 55 µs reflects the more intense shock and effect of inertial membrane opening. Generally, it was noted that the high pressure treated in these cases would produce higher temperatures of the air heated by shock (over 2000 K). For pressures equal to 7.5 and 8.75 MPa, triggering of ignition in the radial channel can be observed at 70 and 62 µs respectively. However, the additional mixing of hot temperature air with the incoming cryogenic hydrogen leads to self-extinction of combustion by the time of 90 µs. This is confirmed by the absence of hydroxyl on the symmetry plane (see Figure 15) and on the 3D domain (see Figure 16). For pressure equal to 9.4 MPa, ignition happens much earlier in the axial channel of the PRD. Larger high temperature zones can be observed in this case, as consequence of the high pressure shock and earlier development of combustion. As shown in Figure 15, a combustion cocoon is formed externally to the TPRD, showing an enhanced reaction outside the top radial channel, conversely to what observed for warm hydrogen at pressure 2.9 MPa. Figure 16 shows the volumetric development of the reacting zone by the hydroxyl mole fraction distribution. It is concluded that pressure equal to 9.4 MPa leads to spontaneous ignition and combustion likely leading to transition into a hydrogen jet flame.

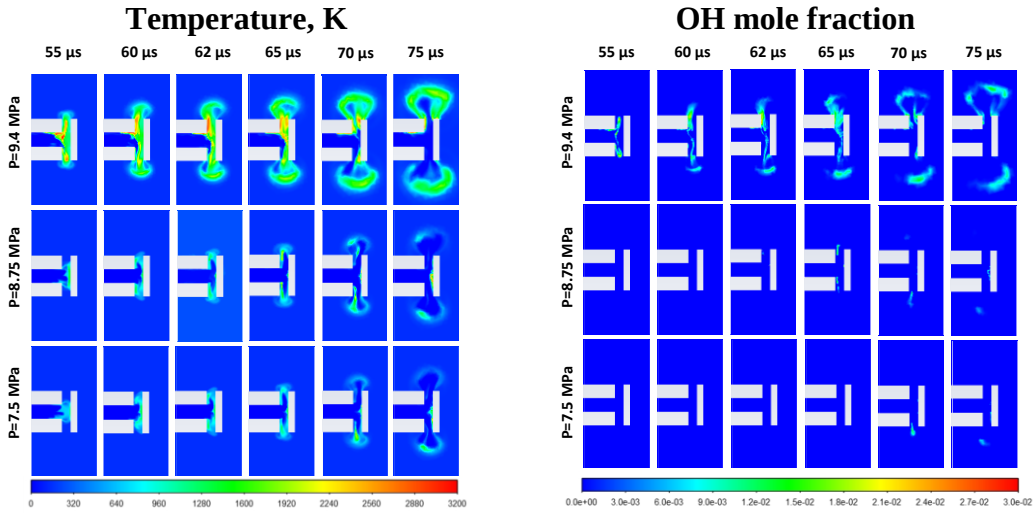

Figure 14. Temperature and hydroxyl mole fraction profiles for P=7.5, 8.75 and 9.4 MPa in time range 55-75 µs. Cryogenic temperature hydrogen (80 K).

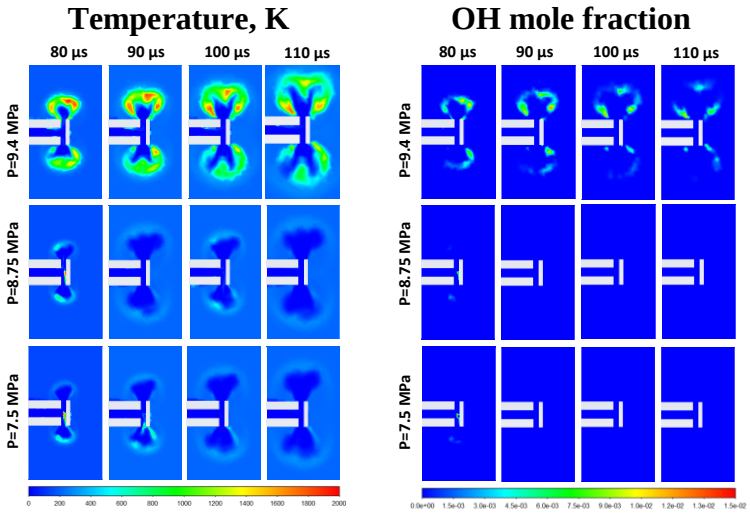

Figure 15. Temperature and hydroxyl mole fraction profiles for P=7.5, 8.75 and 9.4 MPa in time range 80-110 µs. Cryogenic temperature hydrogen (80 K).

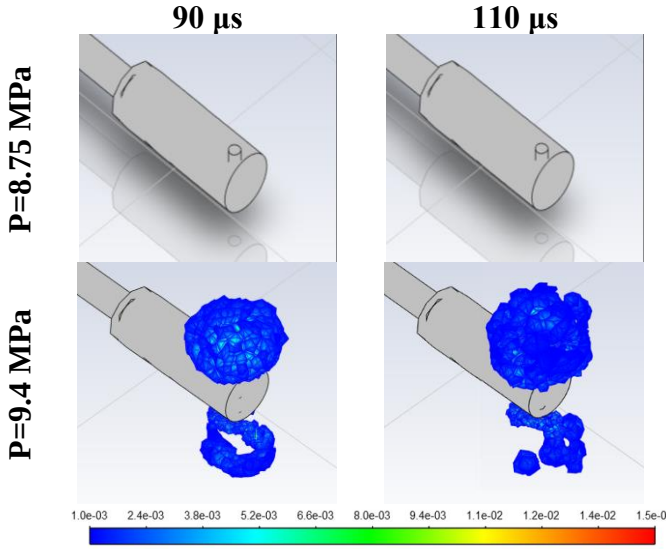

Figure 16. Hydroxyl mole fraction 3D distribution for P=8.75 and 9.4 MPa. Cryogenic temperature hydrogen (80 K).

3.4 Concluding remarks

A LES approach was employed to investigate the effect of hydrogen temperature decrease on pressure limit leading to spontaneous ignition in a T-shaped channel. Ignition and combustion dynamics were assessed in terms of temperature and hydroxyl distributions. For ambient temperature hydrogen (300 K), it was found that a pressure of 2.9 MPa is required to obtain spontaneous ignition and likely transition into jet fire outside the T-shaped channel. Pressure in the range 2.6-2.8 MPa was found to trigger ignition, but later result into self-extinction. A pressure of 2.43 MPa was observed to not trigger ignition. For cryogenic hydrogen (80 K), it was found that a pressure approximately 4 times larger than for warm hydrogen is required to trigger ignition and sustain combustion outside the T-shaped channel, which could likely lead to a hydrogen jet fire. The pressure limit resulted to be 9.4 MPa. Below this pressure, e.g. at 8.75 and 7.5 MPa, numerical simulations results showed that there was ignition in the T-shaped channel which then self-extinguished, as demonstrated by the disappearance of high temperature regions and hydroxyl.

4 Computational study on formation of cryogenic H_2/O_2 mixtures (UU)

CFD simulations are performed to understand the phenomena associated with cryogenic mixtures of H2/O2 and their formation/ignition. The study considers an evaporating pool of liquid hydrogen. The aim of the analysis is to assess how the composition of air in proximity of a hydrogen pool is changing, i.e. if there will be oxygen enrichment because of oxygen condensation, depending on wind conditions. Figure 17 presents a simplified scheme of the problem under analysis.

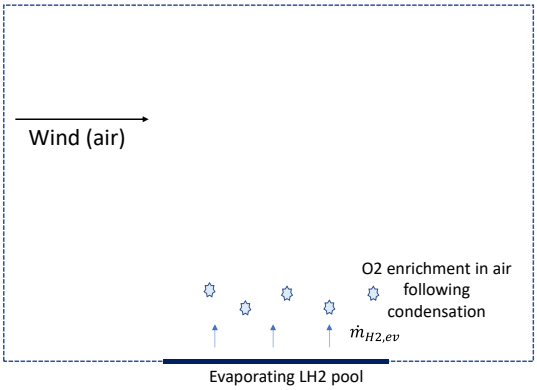

Figure 17. Simplified scheme of the scenario under analysis.

To define the details of the investigated scenario, realistic conditions from (D.Little, 1960)'s experiments were considered to define the mass rate of hydrogen evaporating from the pool. Experimental test on a 120 l spill of LH2 showed that this completely disappeared in 30 s. Density of LH_2 at ambient pressure is 70.85 kg/m^3, thus the mass of spilled hydrogen is about 8.5 kg. This scenario corresponds to an evaporation mass rate $\dot{m}_{H2,ev} = 0.283\ kg/s$. A pool size of 1 m^2 is considered for simulations, leading to a velocity of H_2 of approximately 0.2 m/s. This velocity is imposed as inlet of hydrogen at the pool location with temperature equal to saturation (20.4 K) and ambient pressure. Air with composition 0.21 O_2 by vol and 0.79 N_2 by vol, and temperature 288 K enters the domain at a velocity of 3 m/s. Two directions of the wind are considered: parallel to the pool and 45° tilt towards the pool.

CFD simulations were performed on Ansys Fluent v20.2. The homogeneous mixture model was selected to represent the multiphase mixture and model the condensation of oxygen and nitrogen at temperatures below saturation. The mixture model solves the continuity, momentum and energy equations for the mixture, whereas the volume fraction equation is solved for the secondary phases. A RANS approach was employed to model turbulence. Properties of the mixture components were defined according to NIST chemistry WebBook. The domain has dimensions 4x3x3 m. The 1x1 m pool is located at the centre of the domain. The cell size is 1 cm in proximity of the pool in horizontal direction, whereas it increases from 0.1 mm with a ratio of 1.05 in perpendicular direction to the pool. The total number of control volumes (CV) is 2.58 million. A time step of 4 ms was employed for simulations.

4.1 Results and discussion

Simulation results are used to give insights into the effect of wind direction on the formation of cryogenic hydrogen and condensed oxygen mixtures. Wind velocity is equal to 3 m/s. Figure 18 shows the distribution of hydrogen volume fraction, temperature and liquid oxygen volume fraction. For a wind direction parallel to the pool, it could be observed how the hydrogen cloud is affected by the wind and starts to move along the ground in the wind direction at time 2 s. The low temperature zone is localised in proximity of the pool. Maximum liquid oxygen volume fraction is of the order of 10^{-8}, making it hardly visible in Figure 18. However, the zone with highest volume fraction was observed in simulations towards the ending portion of the pool in the wind direction. At 10 s liquid oxygen volume fraction increased by one order of magnitude. For a wind direction tilted by 45° degrees towards the pool, at time=2s, swirls are produced in the hydrogen distribution. These swirls enhance the entrainment of air into the cold hydrogen flow, as showed by liquid oxygen snapshots at time 10 s, where is clearly visible a zone with volume fraction up to $2.4 \cdot 10^{-5}$. It is possible to conclude that wind direction may affect the potential formation of condensed oxygen phase, even if yet low volume fractions are reached. However, if we look at the concentration of gaseous oxygen (see Figure 19), simulation results for wind direction with 45° angle show a great enrichment by oxygen in the same zone where this is condensing. This would suggest a greater potential for ignition and a following highly energetic event.

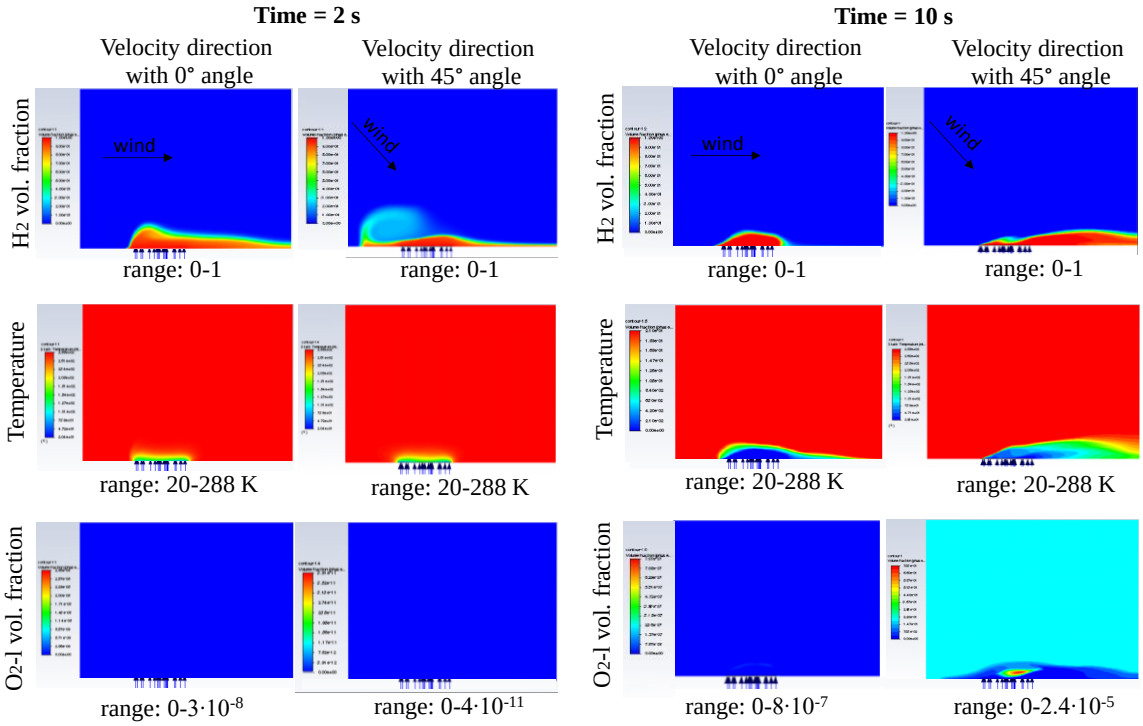

Figure 18. Distribution of hydrogen volume fraction, temperature and liquid oxygen volume fraction at time 2 s and 10 s for two wind directions (wind velocity=3m/s).

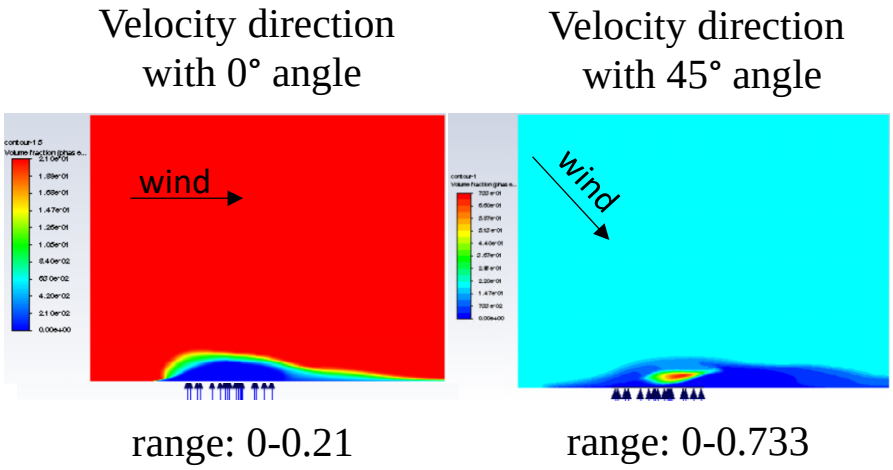

Figure 19. Distribution of gaseous oxygen volume fraction at time 10 s for two wind directions.

4.2 Conclusions

The present CFD study aimed at investigating the condensation of oxygen over an evaporating LH_2 pool and its potential to cause highly energetic events after ignition. The study includes the assessment of the effect of wind parameters on condensation of oxygen.

It is concluded that CFD modelling can be used to investigate the formation of cryogenic hydrogen and condensed oxygen mixtures. CFD simulations can be used to support experimental investigations where it may not be possible to exactly define the underlining cause of highly energetic events following combustion of cold hydrogen/oxygen mixtures.

Simulation results showed that wind parameters affect the potential oxygen condensation. Wind direction tilted by 45° degrees towards the ground was found to lead to a potentially more dangerous scenario compared to wind direction parallel to the ground.

5 References

Bazhenova, T., Bragin, M., Golub, V., Ivanov, M., 2006. Self-ignition of a fuel gas upon pulsed efflux into an oxidative medium. Tech. Phys. Lett. 32, 269–71.

Bell, I.H., Wronski, J., Quoilin, S., Lemort, V., 2014. Pure and Pseudo-pure Fluid Thermophysical Property Evaluation and the Open-Source Thermophysical Property Library CoolProp. Ind. Eng. Chem. Res. 53, 2498–2508.

Benmouffok, M., Freton, P., Gonzalez, J.J., 2018. Theoretical plasma characterization during current pulse. IJRRAS 34.

Bragin, M. V., Makarov, D. V., Molkov, V. V., 2013. Pressure limit of hydrogen spontaneous ignition in a T-shaped channel. Int. J. Hydrogen Energy 38, 8039–8052.

Bragin, M. V., Molkov, V. V., 2011. Physics of spontaneous ignition of high-pressure hydrogen release and transition to jet fire. Int. J. Hydrogen Energy 36, 2589–2596.

Bulewicz, E.M., Sugden, T.M., 1958. The recombination of hydrogen atoms and hydroxyl radicals in hydrogen flame gases. Trans. Faraday Soc. 1855–1860.

Calcote, H.F., Gregory, C.A., Barnett, C.M., Gilmer, R.B., 1952. Spark Ignition. Effect of Molecular Structure. Ind. Eng. Chem. 44, 2656–2662.

Cirrone, D.M.C., Makarov, D., Molkov, V., 2019. Thermal radiation from cryogenic hydrogen jet fires. Int. J. Hydrogen Energy 44, 8874–8885.

D.Little, A., 1960. Final Report on an Investigation of Hazards Associated with the Storage and Handling of Liquid Hydrogen. Report C-61092.

Golub, V. V., Baklanov, D.I., Bazhenova, T. V., Bragin, M. V., Golovastov, S. V., Ivanov, M.F., Volodin, V. V., 2007. Shock-induced ignition of hydrogen gas during accidental or technical opening of high-pressure tanks. J. Loss Prev. Process Ind. 20, 439–446.

Golub, V. V., Baklanov, D.I., Golovastov, S. V., Ivanov, M.F., Laskin, I.N., Saveliev, A.S., Semin, N. V., Volodin, V. V., 2008. Mechanisms of high-pressure hydrogen gas self-ignition in tubes. J. Loss Prev. Process Ind. 21, 185–198.

Golub, V., Volodin, V., Baklanov, D., Golovastov, S., Lenkevich, D., 2010. Experimental investigation of hydrogen ignition at the discharge into channel filled with air. Phys. Extrem. states matter 110–3.

Han, J., Yamashita, H., Hayashi, N., 2011. Numerical study on the spark ignition characteristics of hydrogen e air mixture using detailed chemical kinetics. Int. J. Hydrogen Energy 36, 9286–9297.

Jarosinski, J., Veyssiere, B., 2009. Combustion Phenomena: Selected Mechanisms of Flame Formation, Propagation and Extinction.

Kim, H.J., Hong, S.W., Kim, H.D., 2001. Quenching Distance Measurement for the Control of Hydrogen Explosion. In: International Colloquium on the Dynamics of Explosions and Reactive Systems.

Kuchta, J.M., 1985. Investigation of Fire and Explosion Accidents in the Chemical, Mining, and Fuel-Related Industries A Manual. U.S. Bur. Mines Bull. 680.

Kumamoto, A., Iseki, H., Ono, R., Oda, T., 2011. Measurement of minimum ignition energy in hydrogen-oxygen-nitrogen premixed gas by spark discharge. J. Phys. Conf. Ser. 301.

Lewis, B., Elbe, G. von, 1961. Combustion, Flames and Explosions of Gases, Zeitschrift für Physikalische Chemie. Academic Press, New York.

Ono, R., Nifuku, M., Fujiwara, S., Horiguchi, S., Oda, T., 2007. Minimum ignition energy of hydrogen-air mixture: Effects of humidity and spark duration. J. Electrostat. 65, 87–93.

Proust, C., 2021. PRESLHY D4.4 Summary of experiment series E4.1 results (Ignition parameters).

Spence, D., Woods, B., 1964. A review of theoretical treatments of shock-tube attenuation. J Fluid Mech 19, 161–174.

Terao, K., 2007. Irreversible phenomena. Ignitions, combustion and detonation waves. Springer.

Wolanski, P., Wojcicki, S., 1973. Investigation into the Mechanism of Diffusion Ignition of a Combustible Gas Flowing into Oxidizing Atmosphere. In: Fourteenth Symposium (International) on Combustion. Pittsburgh, pp. 1217–1223.

Yakhot, V., Orszag, S., 1986. Renormalization group analysis of turbulence. I. Basic theory. J. Sci. Comput. 1, 3–51.

Yang, Y., 2011. Plasma discharge in water and its application for industrial cooling water treatment.